View metadata, citation and similar papers at core.ac.uk

brought to you by CORE

provided by IntechOpen

We are IntechOpen, the world's leading publisher of Open Access books Built by scientists, for scientists

4,800
Open access books available

122,000
International authors and editors

135M
Downloads

Our authors are among the

154
Countries delivered to

TOP 1%
most cited scientists

12.2%
Contributors from top 500 universities

CLARIVATE ANALYTICS BOOK CITATION INDEX INDEXED

WEB OF SCIENCE™

Selection of our books indexed in the Book Citation Index in Web of Science™ Core Collection (BKCI)

Interested in publishing with us?
Contact book.department@intechopen.com

Numbers displayed above are based on latest data collected.
For more information visit www.intechopen.com

Chapter 2

Quantitative Separation of an Adsorption Effect in Form of Defined Current Probabilistic Responses for Catalyzed / Inhibited Electrode Processes

Piotr M. Skitał and Przemysław T. Sanecki

Additional information is available at the end of the chapter

http://dx.doi.org/10.5772/53664

1. Introduction

The investigation of organic adsorbate influence on electrode process was started in works of Loshkarev e.g. [1], Schmid and Reilley [2], with theoretical formulation of Weber and Koutecký [3,4]. The problem is described in the book by Heyrovský and Kůta ([5] and literature therein). Later investigations have led to formulation of the *cup pair effect* [6], systematically developed in a series of papers e.g. [7,8]. In our earlier paper [9] it has been shown that catalytic effect of electroinactive organic adsorbate on electrode process can be isolated from CV or NPP faradaic current responses in the form of Gaussian-shaped probabilistic curves (CPR[1]). It turned out that in presence of organic adsorbate showing electrocatalytic effect, the kinetic response can be split into two defined and well shaped responses: one, due to regular reduction of cation and the second one due to reduction catalyzed by an adsorption phenomenon. The latter was named, due to its shape, the *current probabilistic response*. It has been demonstrated that CPR effect can exemplify the visualization and the quantitative measure of organic substance catalytic effect on the electrode process and simultaneously become the picture of adsorption.

The electroinhibition phenomenon was analyzed by means of selected experiments with the use of typical electroinhibitors. As an example a quasi-reversible process of Zn^{2+} electroreduction in the presence of two adsorbates such as n-alkyl alcohols [10] and two cyclodextrins was chosen [11-13,14].

1 Since PCR means Polymerase Chain Reaction and is well established in literature, in the present paper we use the abbreviation CPR.

INTECH
open science | open minds

© 2012 Skitał and Sanecki; licensee InTech. This is an open access article distributed under the terms of the Creative Commons Attribution License (http://creativecommons.org/licenses/by/3.0), which permits unrestricted use, distribution, and reproduction in any medium, provided the original work is properly cited.

So far, the quantitative and qualitative comparison of two systems: without adsorbate (1) and with adsorbate (2) was realized by means of four manners: dividing the adsorption non-affected and affected faradaic currents (1)/(2) or (2)/(1) [5], Tafel plots [10,12], comparison of apparent or individual rate constants [7,8] and/or simple comparison of respective curves, recorded in the presence and absence of organic substance, performed on the same plot [7].

The task of resolution of enhanced or decreased faradaic current response to show the adsorption catalytic/inhibition effect alone has not been undertaken in literature.

The literature analysis indicates that both theoretical and experimental aspects of adsorption at metal solution interface are still developed for both macroscopic and microscopic inhomogeneites (e.g. [15,16] and literature therein). Owing to existing extensive data concerning influence of organic electroinactive substances on electrode process the visualization of adsorption process in an isolated *"pure"* form is needed. It can facilitate the data processing and be competitive or parallel to capacitance currents method. Therefore, in the present paper a number of experimental facts concerning CPR is analyzed. The questions which are answered include: if the CPR approach can be applied to electrode process inhibited by organic substances and if the CPR effect is observed at solid electrodes and/or in nonaqueous media. Moreover, successful attempt to generate CPR effect by numerical simulation with the use of EE model was done.

2. Experimental

The CV, NPP and NPV experiments were carried out with the use of CV50W electrochemical analyzer (BAS, Inc.) and PGSTAT100 voltammetric analyzer (*Autolab Eco-Chemie*) for molecular oxygen reduction. The electrode system was CGME/SMDE type MF-9058 (BAS, Inc.). The mercury drop surface of working electrode was 0.0151 ± 0.0004 cm^2 for CV experiment. The glassy carbon electrodes of working surface 0.0755 ± 0.001 cm^2 (GCE3) as well as 0.0314 ± 0.001 cm^2 (GCE2) were used. For NPP experiments, the drop time was 1.0 s with a pulse-width of 50 ms and sample width 10 ms. In contrary to previous paper data, since eq. (2) contains the element of subtracting of background current, the separate background files are not necessary. The reliability of such simplification was checked by the comparison of CPR curves obtained from residual current corrected and non-corrected data. Obtained differences were not significant for the μA current scale of CPR effect.

Coulometric experiments were carried out with the use of diaphragm electrolyzer on large Hg electrode (of about 12 cm^2 surface), the volume of catholyte was 100 or 80 cm^3. A Pt counter electrode was applied in separated anodic part.

The remaining experimental details concerning DMF solutions were identical with those described in previous paper [17].

http://dx.doi.org/10.5772/53664

3. Kinetics

In modeling of Zn^{2+} electroreduction process the following EE sequence with two one electron steps has been taken into account:

$$Zn^{2+} \underset{k_{-1},\beta_1}{\overset{k_1,\alpha_1}{\rightleftarrows}} Zn^{+} \underset{k_{-2},\beta_2}{\overset{k_2,\alpha_2}{\rightleftarrows}} Zn \quad (1)$$

where: k_1, k_2, k_{-1}, k_{-2} are the heterogeneous rate constants (cm s^{-1}), α_1, α_2, and β_1, β_2 are elementary transfer coefficients of cathodic and anodic process, respectively. In the present paper the extended EE ‖ Hg(Zn) mathematical model described in [18] was applied. For the considered sequence of elementary steps (1), the reversible electron transfer for both electrochemical steps was assumed. In the extended model the considered system consist of two parts: mercury drop area from $r = 0$ to $r = R_0$ and the solution area $r > R_0$. Additionally, it has been assumed that species Zn^{2+} and Zn^{+} dissolve only in electrolyte, whereas metallic zinc dissolve and diffuse only in the mercury phase. It is caused by the fact, that deposited metallic zinc is solution-phobic and has to be immediately pulled into Hg phase to form intermetallic compound (amalgam) spontaneously [18].

The problem formulated above was solved using the *ESTYM_PDE* software. The program was designed to solve and estimate parameters of partial differential equations (PDE) describing one-dimensional mass and heat transfer coupled with a chemical reaction. The validation and comparison with other software are described in [19]. The examples of solving electrochemical problems by means of *ESTYM_PDE* software are described in previous papers [17-27]. The numerical basis of electrochemical simulation is described in references [28-33]. The two types of probabilistic fits with the use of *Origin 7.5* program were applied: the simple Gaussian model $y = y_0 + (A/(w\times(\pi/2)^{1/2}))\times\exp(-2\times((x-x_c)/w)^2)$; the asymmetric double sigmoidal model $y = y_0 + A_m\times(1/(1+\exp(-(x-x_c+w_1/2)/w_2)))\times(1-1/(1+\exp(-(x-x_c-w_1/2)/w_3)))$, where y_0, x_c, A, A_m and (w, w_1, w_2, w_3) are baseline offset, center of the peak, area, amplitude and widths of peaks, respectively.

4. Results and discussion

4.1. The systems with electrode inactive organic adsorbate

The idea [9] of such CPR plots is based on eq. (2):

$$i_{obs}(E) = i_0(E) + i_{ads}(E) \quad (2)$$

where, $i_0(E)$ – faradaic current due to regular (i.e. in absence of adsorbate) electrochemical response, $i_{ads}(E)$ – additional faradaic current due to adsorption effect. It is assumed that the

adsorption process does not change the mechanism of the electrode process, which is in accordance with the literature quoted [1-8,10-13]. In other words, the both currents in eq. (2) represent the same reduction process and the same number of electrons exchanged, moreover their final product is the same as well. The condition should be complete for each considered case.

A representative example of the resolution of deformed by inactive organic adsorbate faradaic current response into components according to eq. (2) is presented in Fig. 1. The visualization of adsorption process in its isolated "*pure*" form is regular and well-designed (Fig.1). The observed adsorption effect is catalytic since the responses (2) and (3) are enhanced and passed in relation to (1) towards positive potential.

The subtraction of experimental currents ($i_{obs}(E) - i_0(E) = i_{ads}(E)$) according to eq. (2) is reasonable since both denote the same electrode process. The applied two-electron Zn^{2+} reduction is not naturally resolved into steps since $k_2 > k_1$ [34] (cf. also the Fig. 10 caption). Therefore, an appearance of adsorption deformed responses (Fig. 1) cannot be explained in terms of resolution of coupled two-electron response. The only assumption is the additivity of currents, according to the rule commonly accepted in electrochemistry.

The two representative sets of the experimental data including five aliphatic alcohols and two cyclodextrins have been selected to establish whether the effect of inhibition can be described by current probabilistic response (CPR). In selection of inhibitors the compounds considered as simple adsorbates (a series of alcohols) as well as complex adsorbates (α,β-cyclodextrins) have been chosen. It has been shown [13] that α-cyclodextrin as inhibitor can form a condensed film. Both of the selected groups of compounds are known as electrode process inhibitors [7,10-13,35,36]. Moreover, the influence of eight additional organic adsorbates has also been investigated in connection with another electrode processes (see further).

The mechanism of Zn^{2+} electroreduction and the physical model of the inhibitors influence were proposed in quoted literature. It was shown that zinc electroreduction can be considered as successive two electron transfer steps (e.g., [37-40]). The results obtained by Fawcett and Lasia [34,41] in non-aqueous media in the presence of tetraalkylammonium perchlorates, especially in dimethylsulfooxide, revealed the complex, nonlinear potential dependence of experimental rate constant (c.f. also Fig. 1 in [41] for dimethylformamide). It indicates that the reaction consists of at least two steps. In dimethylsulfooxide the standard rate constant of the second step is greater than that of first one [34]. It means that E_0 potential of Zn^{2+}/Zn^{+} couple should be more negative than that of hypothetical Zn^{+}/Zn^{0} one. The similar conclusion is given in paper by Manzini and Lasia [40]. Additionally, it was stated that "*coulometric measurments indicate 100% yield and no metal was found in the solution after electrolysis*" [34]. It is not surprising since metallic zinc is solution-phobic and must be immediately pulled into Hg phase to form an intermetallic compound (amalgam).

http://dx.doi.org/10.5772/53664

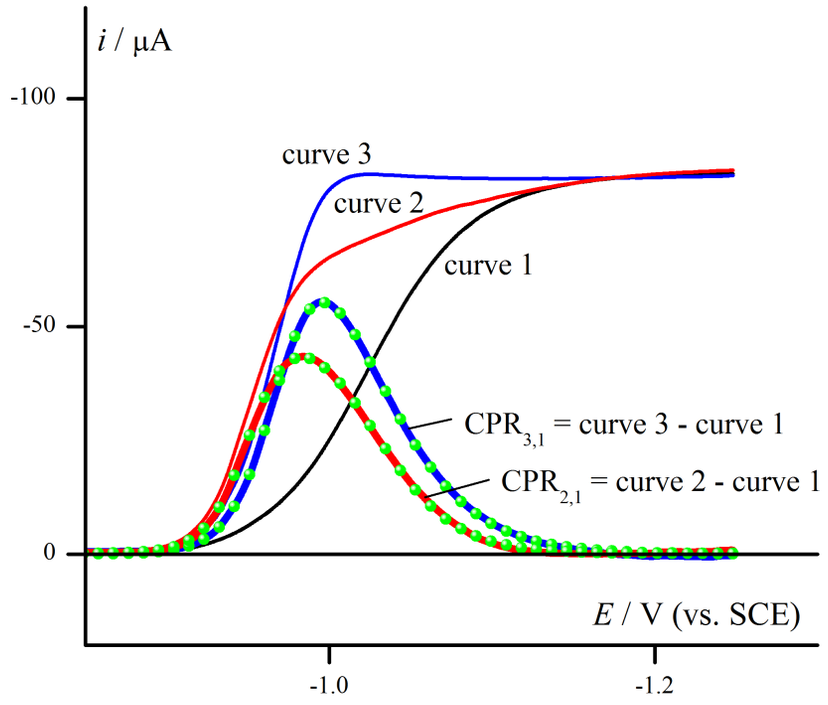

Figure 1. Experimental results expressing the idea of CPR effect. Electroreduction of Zn^{2+} in absence and presence of inert adsorbate. Regular-shaped NPV response (curve 1) and adsorption deformed NPV responses (curves 2 and 3). The difference between regular (1) and deformed response (2) or (3) is a quantitative measure of adsorption influence i.e. CPR effect: curve 3 minus curve 1 as well as curve 2 minus curve 1. Experimental conditions: NPV electroreduction of 1 mM Zn^{2+} in 1 M $NaClO_4/H_2O$ solution on Hg electrode in presence of an adsorbate: (2) – 5 mM *N,N'*-dimethylthiourea; (3) – 0.2 mM 3,4-diaminotoluene. CPR responses were approximated with the probabilistic theoretical model: points (green) are a asymmetric double sigmoidal fits. The values of parameters for $CPR_{2,1}$: $y_0 = -1.35\times10^{-7}$, $x_c = -0.989$, $A = 5\times10^{-5}$, $w_1 = 0.076$, $w_2 = 0.025$, $w_3 = 0.013$, $\chi^2 = 7.7\times10^{-14}$, $R^2 = 0.9996$ and for $CPR_{3,1}$: $y_0 = -1.54\times10^{-8}$, $x_c = -0.995$, $A = 1\times10^{-4}$, $w_1 = 0.049$, $w_2 = 0.031$, $w_3 = 0.014$, $\chi^2 = 1.3\times10^{-13}$, $R^2 = 0.9995$.

Since the pure reversible EE process of Zn^{2+} reduction is not observed in practice, there must be a reason for quasi-reversibility in form of slow step. Fawcett and Lasia [41] suggested the model in which the two step reduction is complicated by slow adsorption process of substrate and its transfer to the electrode, similarly as it was proposed for reduction of Na^+, Li^+ [42] and Ca^{2+}, Sr^{2+}, Ba^{2+} cations [43]. In the case when the dehydration desolvatation of zinc cations were considered as chemical steps [37,40], another explanation of the quasi-reversibility is provided by the presence of such preceding slow elementary processes or the situation in which electron transfer is coupled with slow desolvation.

Our results obtained in 1.0 M $NaClO_4$ solution revealed $i_p/v^{1/2} = f(v)$ dependence decreasing with scan rate v which suggests that the reduction process must be complicated by a slow step.

According to our assumption, the EE mechanism (1), i.e. the sequence of two consecutive steps $Zn^{2+} \xrightarrow{e} Zn^{+} \xrightarrow{e} Zn$, remains the same on both covered and uncovered electrode where intermediate Zn^+ is stabilized by hydration, and undergoes fast electrochemical reduction. The analogical assumptions have been undertaken in relation to Cd^{2+} electroreduction [44]. Since the CPR effect is based on comparison of the two reductions, namely in absence and

presence of organic adsorbate, an extensive mechanistic analysis at the moment is not decisive for our purpose.

Our coulometric measurements were performed at sufficiently negative potentials diffusion region in order to avoid the participation of the anodic current, and gave the number of electrons exchanged 2.02 ± 0.05 for 1 mM Zn^{2+} and 1 M $NaClO_4$ solution. In the presence of two representative adsorbates the obtained results were 2.00 ± 0.09 for *n*–pentanol (0.1 M) and 1.92 ± 0.05 for α-cyclodextrin (0.01 M).

The representative results of applying the CPR approach to inhibition are presented in Fig. 2A and 2B. It is striking that simple, according to eq. (2), subtraction of respective parent matrices recorded in presence and absence of inhibitor (or catalyst – Fig.1), provides the curves which are elegant and defined in shape. Very similar picture is observed once convoluted CV responses are considered. The Gaussian fit done for those curves is of good or even very good quality, which justifies the use of the adjective probabilistic. None of the experimental parent curves in this paper has been idealized by smoothing or other similar procedures.

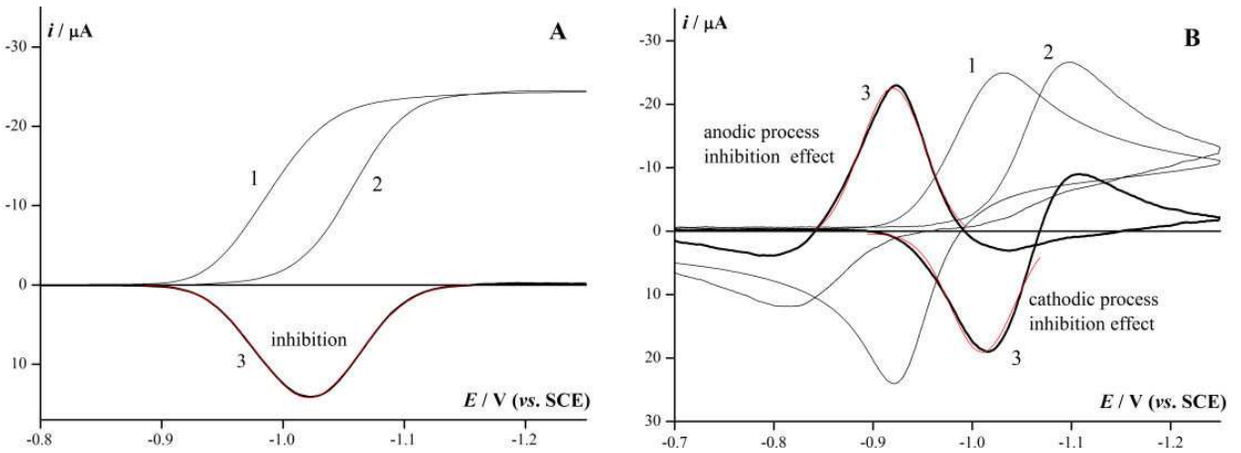

Figure 2. The separation and visualization of experimental *n*-pentanol adsorption / inhibition effect according to eq. (2). The electrode process: electroreduction of 1 mM Zn^{2+}, 1M $NaClO_4$ on Hg electrode in absence (curve 1) and in presence (curve 2) of *n*-pentanol. Curve 3 (*current probabilistic response* (CPR)) displays the inhibition effect alone in form of $i_{c,\,ads}$ (E). All currents are in the same scale. Red curve is a Gaussian fit. (A) NPP technique. The values of Gaussian fit parameters are: $y_0 = -1.05\times10^{-7} \pm 2.8\times10^{-8}$, $x_c = -1.0209 \pm 0.0001$, $w = 0.0844 \pm 0.0003$, $A = 1.51\times10^{-6} \pm 6.9\times10^{-9}$, $\chi^2 = 1.02\times10^{-14}$, $R^2 = 0.9996$. (B) CV technique. Scan rate 1.003 V s^{-1}. The Gaussian fit (red curves) results in good correlation parameters. The values of R^2 parameter of Gaussian fit are 0.9763 and 0.9928 for the cathodic and anodic part, respectively.

Data presented in Fig. 3 indicate the increasing influence of aliphatic alcohols on the electrode process depending on the increasing, from *n*-propanol to *n*-hexanol, length of carbon chain, similarly as it was described in the literature [10].

The similar picture is observed for two cyclodextrins (Fig. 4A,B), another typical object in investigations of electrode process inhibition [11-13].

http://dx.doi.org/10.5772/53664

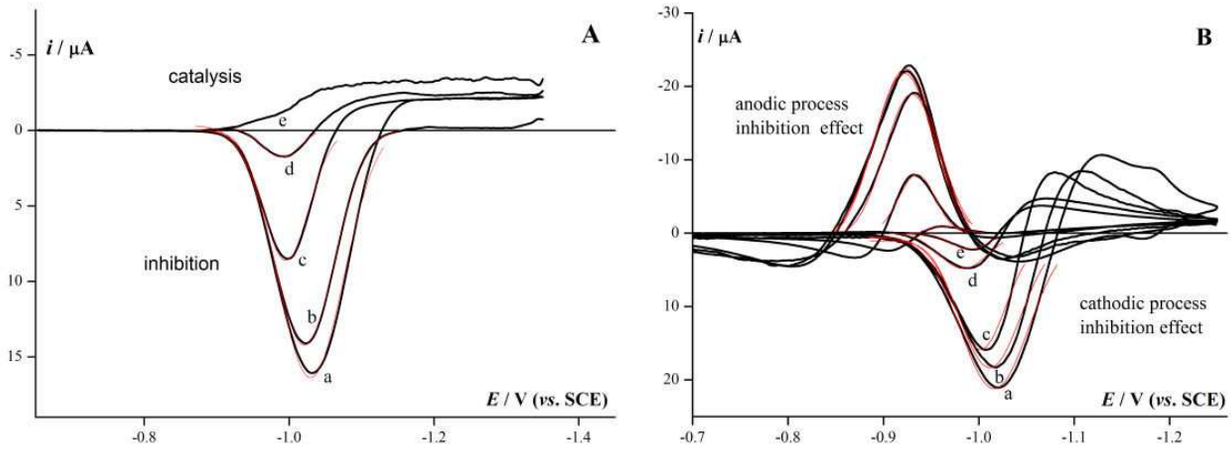

Figure 3. A comparison of experimental CPR electroinhibition effects, determined for five aliphatic alcohols from eq. (2) for electroreduction process of 1 mM Zn^{2+} in 1 M $NaClO_4$ on Hg electrode: (a) saturated ≈ 0.06 M *n*-hexanol, (b) 0.1 M *n*-pentanol, (c) 0.1 M *t*-pentanol, (d) 0.1 M *n*-butanol, (e) 0.1 M *n*-propanol. The parent NPP responses are not shown. (A) NPP technique. The Gaussian fit (red curves) results in good correlation parameters, for example the values of R^2 parameter are: (a) R^2 = 0.9949; (b) R^2 = 0.9996; (c) R^2 = 0.9942; (d) R^2 = 0.9823. (B) CV technique. Scan rate 1.003 V s^{-1}. The Gaussian fit (red curves) results in good correlation parameters for example, the values of R^2 parameter of Gaussian fit for cathodic process are: (a) R^2 = 0.9848; (b) R^2 = 0.9756; (c) R^2 = 0.9649; (d) R^2 = 0.9740; (e) R^2 = 0.9656. The values of R^2 parameter for anodic process (a) R^2 = 0.9950; (b) R^2 = 0.9891; (c) R^2 = 0.9913; (d) R^2 = 0.9781; (e) R^2 = 0.9243.

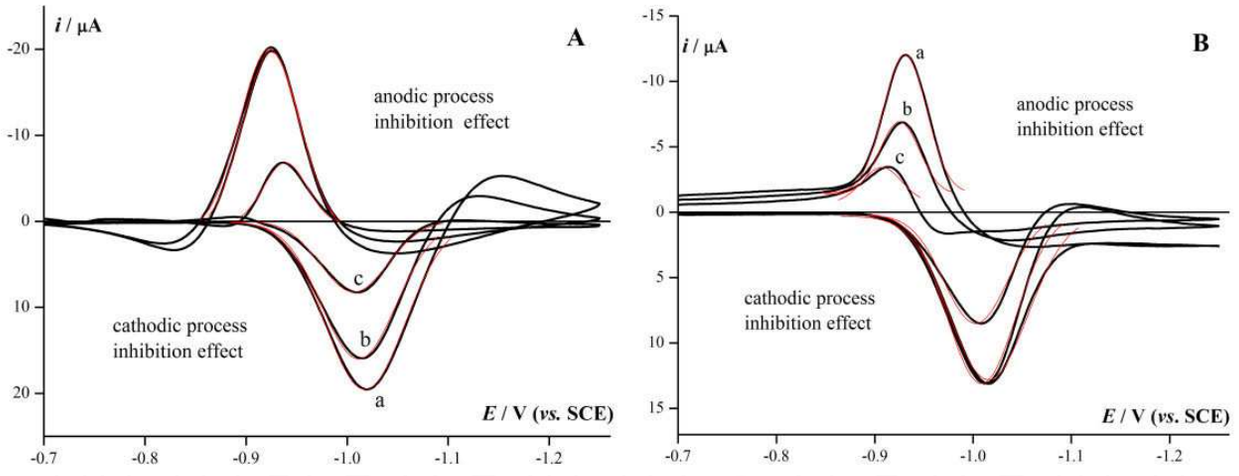

Figure 4. A comparison of experimental electroinhibition effects of CPR type, determined from eq. (2) for different concentrations (a) 0.1 M, (b) 0.05 M, (c) 0.01 M of *α*-cyclodextrin (A) and *β*-cyclodextrin (B). The parent electrode process: CV electroreduction of 1 mM Zn^{2+} in 1M $NaClO_4$ on Hg. Scan rate 1.003 V s^{-1}. (A) The Gaussian fit (red curves) results in good correlation parameters, for example the values of R^2 parameter of Gaussian fit for cathodic process are: (a) R^2 = 0.9956; (b) R^2 = 0.9920; (c) R^2 = 0.9946. The values of R^2 parameter for anodic process are: (a) R^2 = 0.9972; (b) R^2 = 0.9995; (c) R^2 = 0.9905. (B) The Gaussian fit (red curves) results in the good correlation parameters for example the values of R^2 parameter of Gaussian fit for cathodic process are: (a) R^2 = 0.9936; (b) R^2 = 0.9914; (c) R^2 = 0.9804. The values of R^2 parameter for anodic process are: (a) R^2 = 0.9861; (b) R^2 = 0.9479; (c) R^2 = 0.8379.

The results indicate that the influence of cyclodextrins on the electroreduction process is not uniform and that α–CD is effective as an inhibitor, which remains in agreement with litera-

ture data [12]. The data presented in Fig. 3 for alcohols and in Fig. 4 for cyclodextrins have shown, that it is possible to obtain the picture of inhibitory effect more pronounced than in case of applying the single value of kinetic parameter e.g. k_{app} or k_1, k_2 alone. The Gaussian fit is also included for data in Fig. 3 – 4. It is evident that fully shaped curves are obtained for relatively high concentration of the adsorbate. The quality of Gaussian fit decreases with the lowering of the adsorbate concentration as it could have been expected.

The detailed investigations with the use of cyclodextrins as adsorbates have shown that the adsorption process is complex with the possibility of compact layers or multi-layers, host-guest complexes formation [13]. Our results with good quality Gaussian fit suggest that both complex (α, β-cyclodextrins) and simple adsorption (alcohols) undergo Gaussian distribution.

Application of CV method usually leads to a series of peaks corresponding to the different scan rates and so it is in our case. However, CV currents recorded at different scan rates are not comparable and should be normalized by $v^{1/2}$ factor. The different scan rate data, performed in such a way, are presented in form of *CPR* curves in Fig. 5. In other words, instead of parent CV peaks for regular and inhibited process, the final *CPR* curves can be taken under consideration.

On the other hand, the $Q = f(v)$ plot (Fig. 6A) makes it possible to express the inhibition effect quantitatively and normalization by $v^{1/2}$ factor is not needed. In turn, the dependence of the relative inhibition effect $(Q_{CD} - Q_{Zn})/Q_{Zn}$ (where Q_{Zn}, Q_{CD} are charges obtained from integrated cathodic parts of CV curves for electroreduction of Zn^{2+} 1 mM in 1 M $NaClO_4$ in absence and presence of α,β-CD, respectively) at different concentrations and scan rates is presented in Fig. 6B.

Apart from better visualization and separation of adsorption effect from "mixed" current response, CPR approach gives the possibility of adsorption isotherm determination. A respective attempt is presented in Fig. 6B. An assumption was made that a charge Q_{CD} determined from CPR curve is proportional to the amount of adsorbed species. The similar assumption is commonly accepted when adsorption phenomena are investigated by differential capatitance method. A change ∂C is assumed to be proportional to ∂Q and to Γ. The results of Langmuir fit indicate that the obtained parameters are reasonable in the range of the published data [41].

The coincidence with the Gaussian function is expected not to be specific for studied system Zn^{2+}/alcohols and Zn^{2+}/cyclodextrin. It should be observed for at least other qusireversible-irreversible reduction/inert organic adsorbate systems in which pre-peaks or post-peaks do not appear.

It is very probable that numerous factual current responses (CR) and not only curves affected by the effects of inhibition, lead to similar CPR curves with almost identical shapes. Consequently, any change in electrochemical response caused by the influence of added adsorbate, complexing agent or other factors is manifested by, at least, the following influences: positive/negative shift of CR along potential axis and/or change of the CR slope and/or decrease/increase of its high. Above effects occur together, but usually one of them domi-

http://dx.doi.org/10.5772/53664

nates. Therefore, the observed CPR effect, that is an output function, must be interpreted in frames of its parent experimental input.

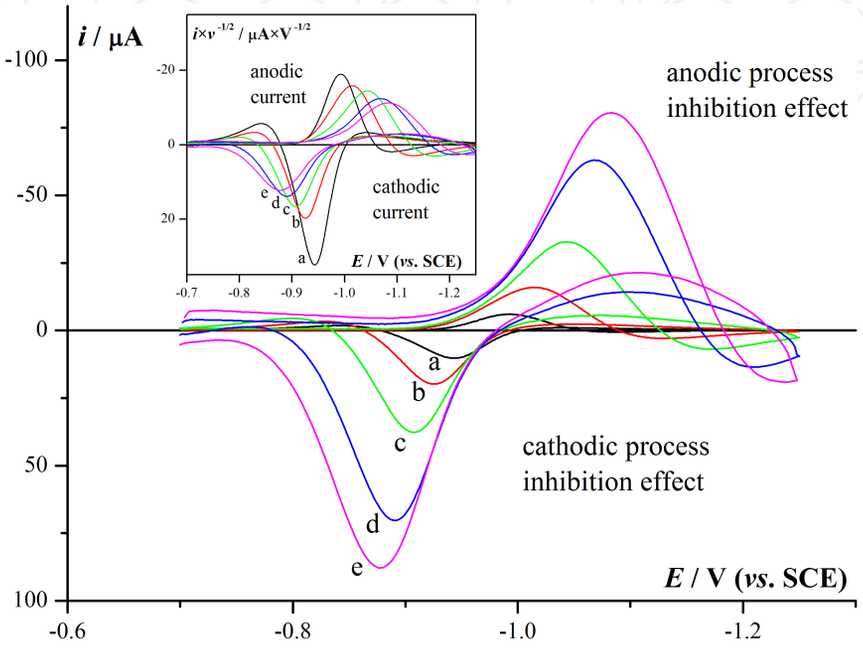

Figure 5. A comparison of experimental electroinhibition effect of CPR type for 1 mM Zn^{2+}, 1 M $NaClO_4$, 0.05 M *α* –CD on Hg electrode at different scan rate in V s^{-1}: (a) 0.1, (b) 1.003, (c) 5.12, (d) 25.6, (e) 51.2. Gaussian fits for a,b,c,d,e plots, not shown on the plot, are of very good quality by statistics. The normalized ($ix v^{-1/2}$) currents of CPR curves are shown in the additional sub-window. The parent CV responses are not shown.

Another experimental examples of CPR effects by CV and NPV techniques are presented in Fig. 7 and Fig. 8 for various adsorbates and various electrode processes.

Data of Fig. 8 A and B present the influence of added organic adsorbates as thiourea (part A, A') and *N,N*-dimethylaniline (part B, B') on molecular oxygen electroreduction in DMF and water, respectively. Fig. 9 presents the case in which the influence of substituent on adsorbate molecule on fixed electrode process is visible. The catalytic effect increases once the electron density on nitrogen atom in thiourea increases. The effect on substituent on thiourea molecule on apparent rate constant is described in paper by Ikeda and co-authors [45].

The results indicate that CPR effect is observed also on GCE and in nonaqueous medium (Fig. 8A).

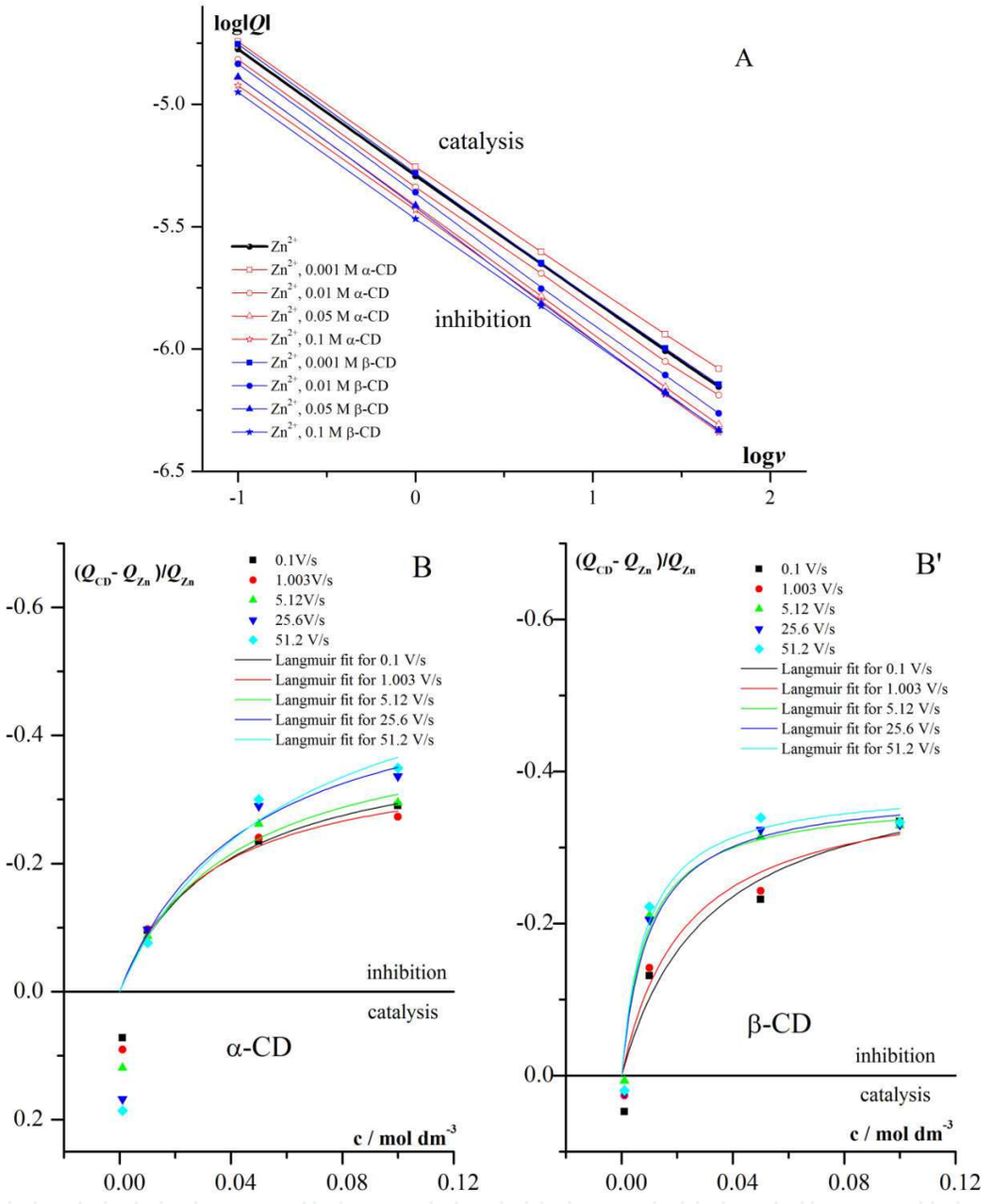

Figure 6. (A) The logarithmic dependence of the charge obtained by integration of cathodic scans of experimental CV curves for 1 mM Zn^{2+}electroreduction in 1.0 M $NaClO_4$ on Hg electrode in absence and presence of *α*-CD and *β*-CD against scan rate. Note that for low 0.001 M concentration of *α*-CD and *β*-CD the inhibition effect changes into the catalytic effect (two lines above thick black line for Zn^{2+} reduction alone refer to catalysis). (B) The normalized CPR effect presented in form of adsorption isotherm obtained on the basis of respective integrated current responses. The scatter plots represent the dependence of the relative inhibition effect for CV electroreduction of Zn^{2+} 1 mM in 1M $NaClO_4$ on Hg electrode in function of *α*-CD and *β*-CD concentration at different scan rates. Q_{Zn}, Q_{CD} – charges obtained from integrated cathodic parts of CV curves. The curves represent the Langmuir fit in form of eq.: $q = q_s Kc/(1+Kc)$, where q, q_s – surface excess, surface excess at saturation and K – equilibrium constant of adsorbate at surface. The examples of values of parameters of Langmuir fit for *α*-CD: at v = 0.1 V s^{-1}; $q_s = -0.40 \pm 0.19$, $K = 27 \pm 33$, $\chi^2 = 3.5\times10^{-3}$, $R^2 = 0.911$; and for *β*-CD: at 51.2 V s^{-1}; $q_s = -0.38 \pm 0.05$, $K = 113 \pm 71$, $\chi^2 = 2.2\times10^{-3}$, $R^2 = 0.949$. Note that for low concentrations of *α*-CD and *β*-CD inhibition effect changes into catalytic effect. The effect shape of plot resembles the Langmuir plot.

http://dx.doi.org/10.5772/53664

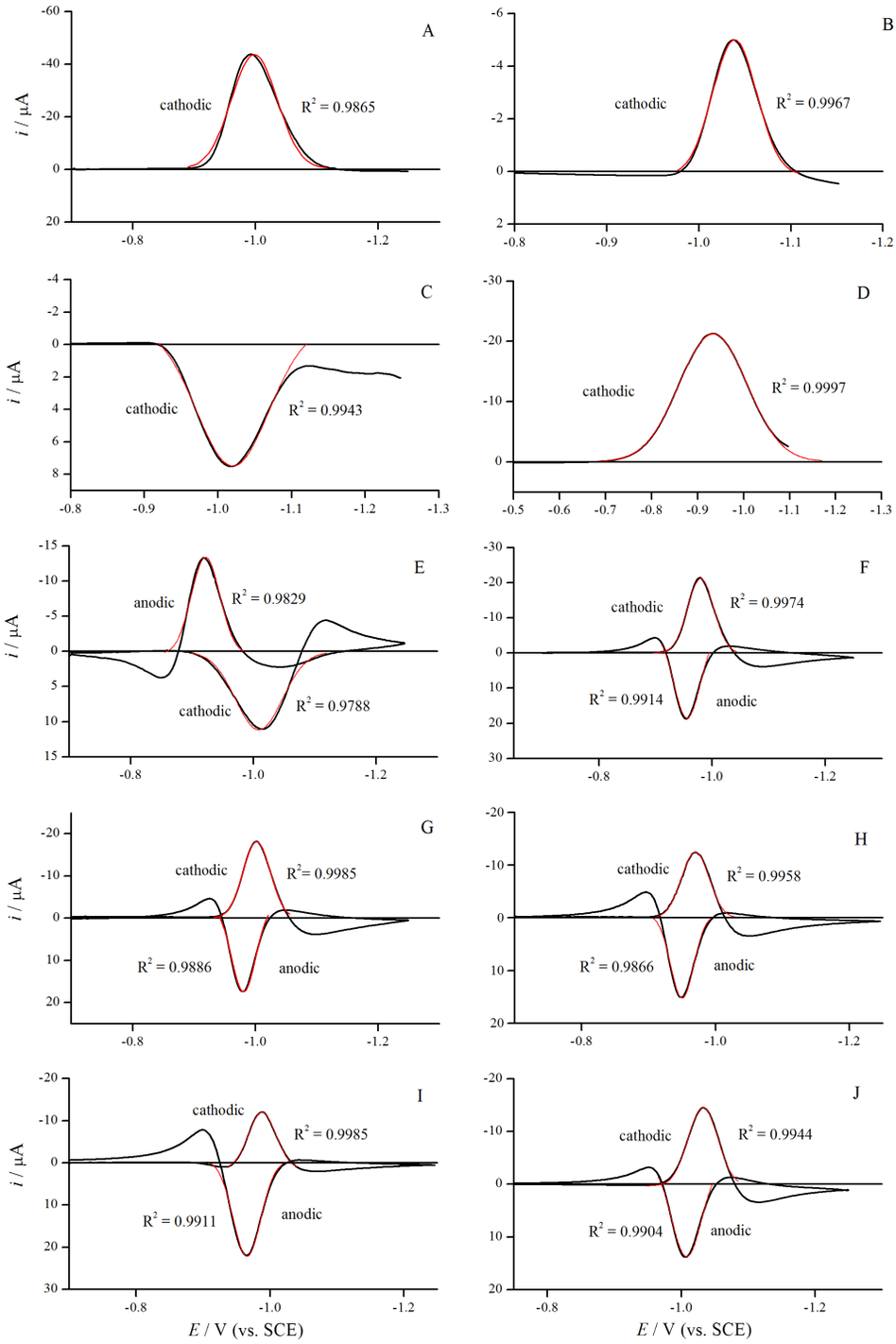

Figure 7. A–J. Examples of CPR results (parent responses are not shown) for different electrode process/adsorbate systems obtained with the use of CV and NPV techniques. (Plots A-C): The NPV electroreduction of 1 mM Zn^{2+} in 1 M $NaClO_4$ in H_2O on Hg electrode in presence: (A) – 5 mM *N,N'*-dimethylthiourea; (B) – 5 mM *N,N,N',N'*-tetramethylthiourea; (C) – 2 μM dextran. (Plot D): The NPV electroreduction of molecular oxygen about 4 mM in 0.3 M TBAP in DMF on GCE3 in presence 1 mM *N,N*-dimethylaniline. (Plots E-J): The CV electroreduction of Zn^{2+} in 1 M $NaClO_4$ in H_2O on Hg electrode in presence of: (E) – 10 μM dextran; (F) – 2 mM 3,4-diaminotoluene; (G) – 55 mM thiourea; (H) – 5 mM *N,N'*-dimethylthiourea; (I) – 5 mM *N,N'*-diethylthiourea; (J) – 5 mM N,N,N',N'-tetramethylthiourea. Scan rate 1 V s^{-1}. The Gaussian fit (red curves) and the values of R^2 correlation parameter are shown on the plot.

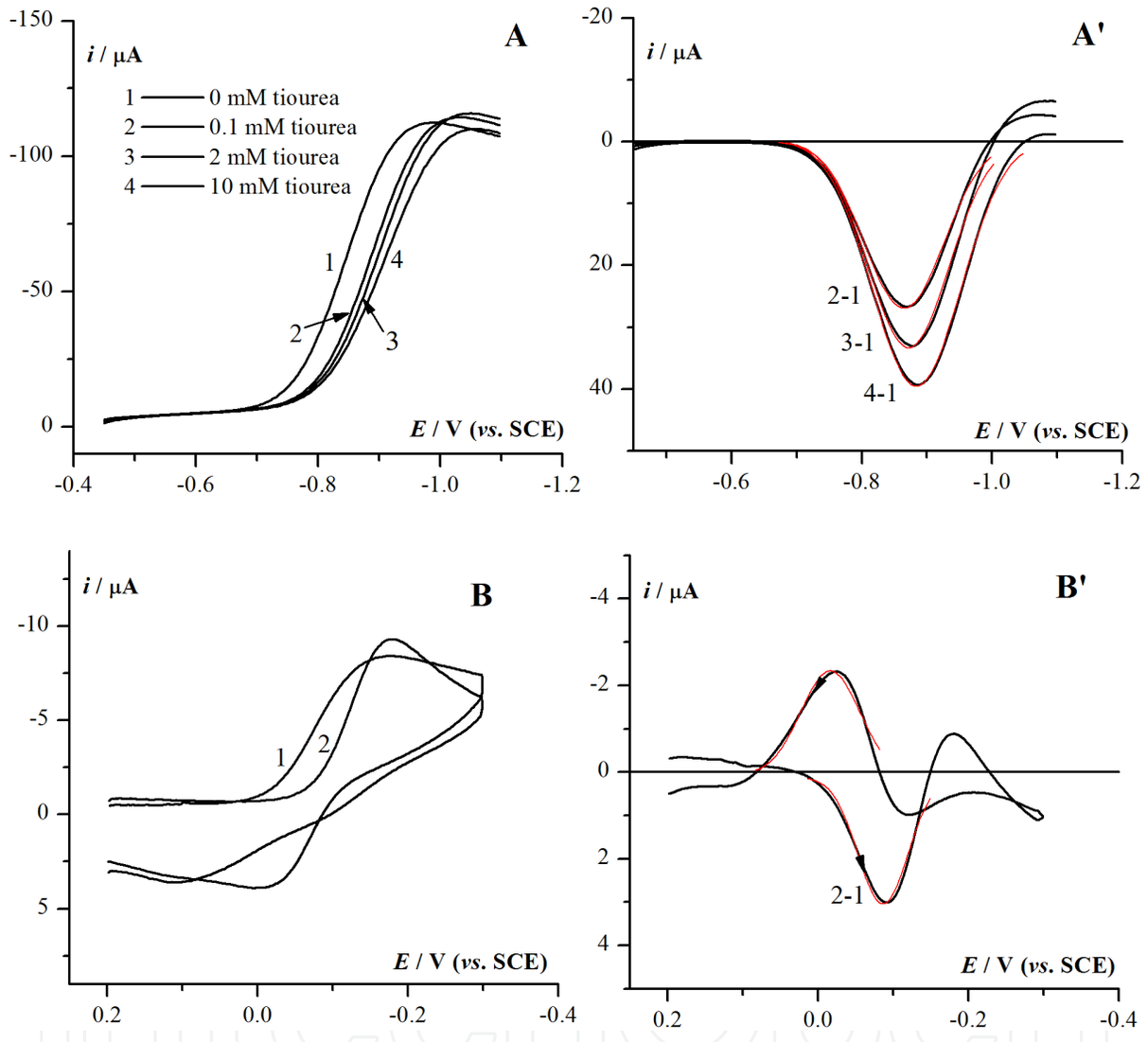

Figure 8. Further experimental examples of CPR inhibition effect. (A) The effect of thiourea on one-electron normal pulse voltammetry reduction of molecular oxygen in 0.3 M TBAP in DMF on GCE3. Thiourea concentration 0, 0.1, 2, 10 mM, O_2 concentration about 4 mM. (A) The same data in CPR form. The Gaussian fit (red curves) leads to good correlation parameters. For example the values of R^2 parameter of Gaussian fit are: (2–1) $R^2 = 0.9926$; (3–1) $R^2 = 0.9913$; (4–1) $R^2 = 0.9920$. (B) The effect of *N,N*-dimetyloaniline on two-electron electroreduction of molecular oxygen by CV in 0.2 M KNO_3 in H_2O on Hg electrode. Scan rate 1 V s^{-1}, *N,N*-dimetyloaniline concentration 1mM, O_2 concentration about 1 mM. (B′) The same data in CPR form. The Gaussian fit (red curves) results in the good correlation parameters. For example the values of R^2 parameter of Gaussian fit are 0.9738 and 0.9628 for cathodic and anodic process, respectively.

http://dx.doi.org/10.5772/53664

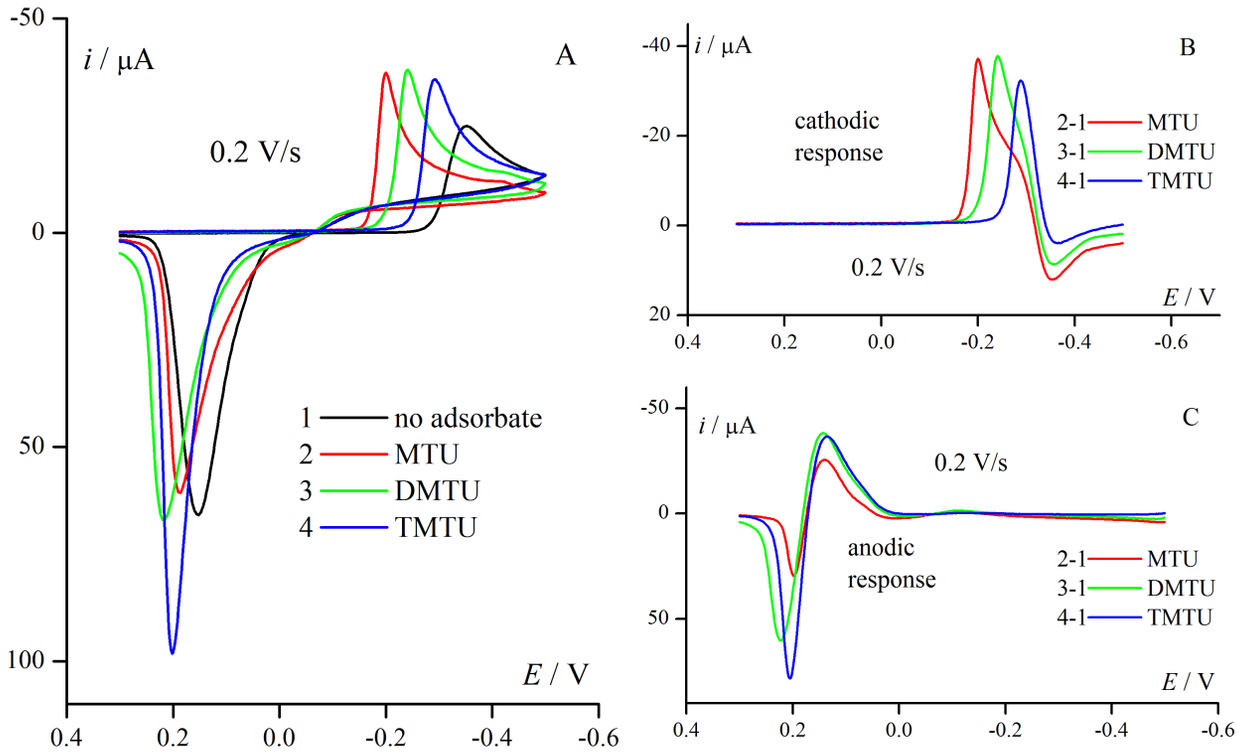

Figure 9. Further examples of CPR effect. Electroreduction of 1 mM Bi^{3+} in 0,1 M $HClO_4$ on GCE2 in presence and absence of 10 mM substituted thioureas (N-methylthiourea (MTU), N,N'-dimethylthiourea (DMTU), N,N,N',N'-tetramethylthiourea (TMTU)). The increase of the catalytic substituent effect from MTU through DMTU to TMTU is visible on position and height of cathodic responses. Scan rate 0.2 V s^{-1}. The parent CV responses are not shown.

4.2. CPR effect as a result of theoretical model

Since the presented results are only an experimental and fenomenological view of the problem, the respective theoretical background is needed. It turned out that the Gaussian-shaped curves of *CPR* type can be obtained also theoretically by numerical simulation. We used the theoretical kinetic EE ‖ Hg(Zn) model and *ESTYM_PDE* software, both described in *Kinetics* section. The literature values of kinetic parameters determined for Zn^{2+} electroreduction in the 1 M sodium perchlorate solution [18] were applied. The EE mechanism provides the simple but reliable model among others proposed for Zn^{2+} electroreduction [38,39,46-49]. The results of simulation are presented in Fig. 10. It turned out that increase/decrease of electrochemical rate constant corresponds to a change of CV curve which is identical to Gaussian *CPR* experimental curve. For clarity, the results of Gaussian fit are shown separately in Fig. 10B. The obtained results of performed simulation provide an indirect evidence of assumption commonly applied in literature that electrocatalysis/electroinhibition effect can be described by increase/decrease of heterogeneous rate constant [15]. The simulations

confirm the literature adsorption model in which the effective observed current is the superposition of both currents on the free surface and on covered fraction i.e. "adsorption" current. It is assumed that the rate constants on covered and uncovered surface should be different (Fig. 10 – simulation). Moreover, the resolution of the experimental currents for two reductions gives possibility for calculation of individual rate constants. It has to be noticed, however, that the mathematical analysis described in reference [50] indicates that the effects of inhibition can be much more complex than a simple k_s decrease analysis presented in Fig. 10.

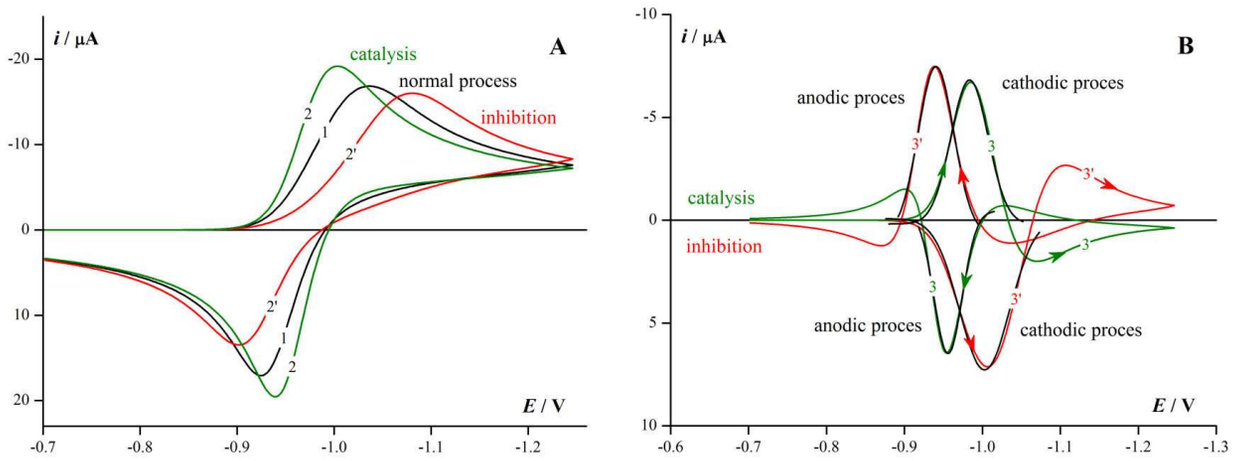

Figure 10. (A) An example of CV simulation results obtained for EE ‖ Hg(Zn) mechanism (section *Kinetics* eq.(1)) with the following kinetic parameters: v = 1.0 V s^{-1}, $D_1 = D_2$ = 4. 0×10^{-6} cm^2s^{-1}, D_3 = 1.67×10^{-5} cm^2s^{-1}, $E_{0,1}$ = –1.049 V $E_{0,2}$= –0.904 V, A = 0.0159 cm^2 (spherical electrode), $\alpha_1 = \alpha_2$ = 0.67; (1) $k_1 = k_{-1}$ = 0.031, $k_2 = k_{-2}$ = 0.35; (2) $k_1 = k_{-1}$ = 0.09, $k_2 = k_{-2}$ = 0.9; (2′) $k_1 = k_{-1}$ = 0.01, $k_2 = k_{-2}$ = 0.1 (rate constants in cm×s^{-1}); the values of kinetic parameters were taken from [18]. Initial concentration of substrate was c_0 = 1 mM. Curves 1, 2 and 2′ were obtained from the simulated CV curves for normal process, electrocatalysis and electroinhibition, respectively. (B) Curves 3 (green) and 3′ (red) represent the *Gaussian current response* and were obtained from the simulated CV curves (A) for electrocatalysis and electroinhibition effect, respectively. The Gaussian fits (black curves) result in good correlation parameters. For example the values of R^2 parameter for curve 3 for cathodic and anodic process are 0.9776 and 0.9848 respectively; for curve 3′ for cathodic and anodic process R^2 values are 0.9770 and 0.9896, respectively.

Despite the fact that the results of modeling of the CPR effect have been presented (Fig. 10), this paper is based mainly on experimental facts. Deeper theoretical analysis of observed phenomena is not possible at the present state of knowledge.

4.3. The CPR effect obtained from processed literature data

In order to extend the scope of experimental data concerning CPR effect, the CPR effect obtained from processed literature data [5,14,51] is presented in Figs. 11-14. The influence of added organic adsorbate, namely polyvinyl alcohol, on VO^{2+} reduction is shown in Fig. 11 A and A' (source of data: [5b]).

http://dx.doi.org/10.5772/53664

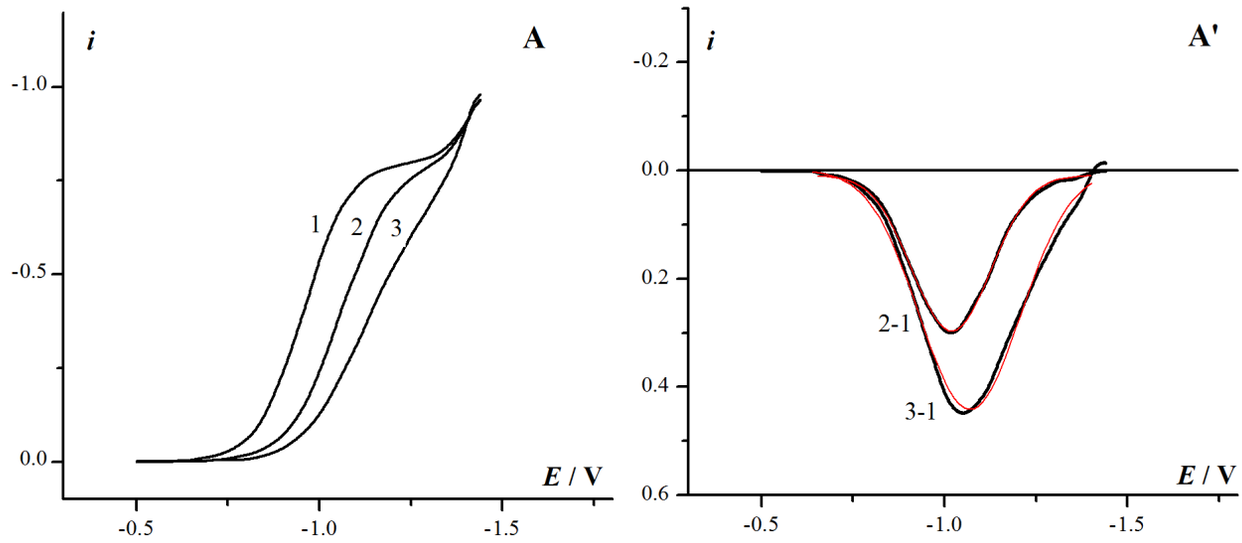

Figure 11. Further experimental examples of CPR inhibition effect derived by digitalization and processing of literature data. (A) The effect of polyvinyl alcohol on the reduction of VO^{2+}. Curve (1) – 3 mM $VOSO_4$, 0.1 M H_2SO_4. Polyvinyl alcohol concentration: (2) – 0.005%, (3) – 0.0075%. Source of data [5b]. (A') The same data in CPR form. The Gaussian fit (red curves) leads to good correlation parameters. For example the values of R^2 parameter of Gaussian fit are: (2–1) $R^2 = 0.9988$; (3–1) $R^2 = 0.9930$.

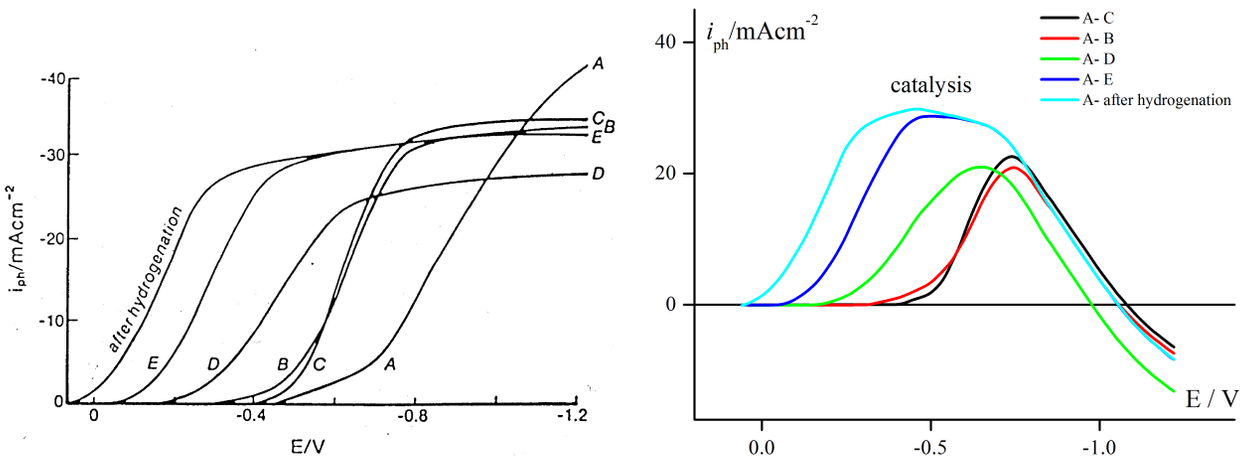

Figure 12. Examples of CPR effect (right plot) derived by digitalization and processing of literature data (left plot) concerning photocurrent-potential relation for p-Si electrode (Fig. 1 p. 206, [51], with kind permission from Springer Science+Business Media B.V.). The similar picture (not shown) can be obtained basing on Fig. 4, p. 208, in monograph [51]. Symbols ABCDE denote the surface etching procedure described therein.

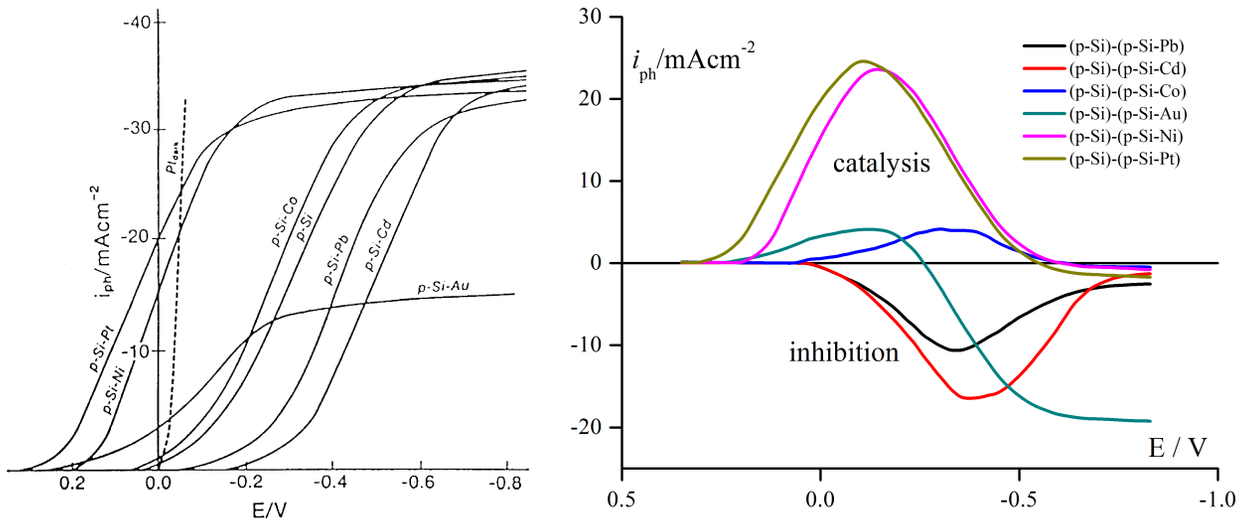

Figure 13. Examples of CPR effect (right plot) derived by digitalization of literature data (left plot) covering potentiodynamic runs recorded for p-Si and p-Si-Me electrodes (Fig. 3 p. 207, [51], with kind permission from Springer Science +Business Media B.V.). The similar picture (not shown) can be obtained basing on Fig. 5, p. 208, in monograph [51].

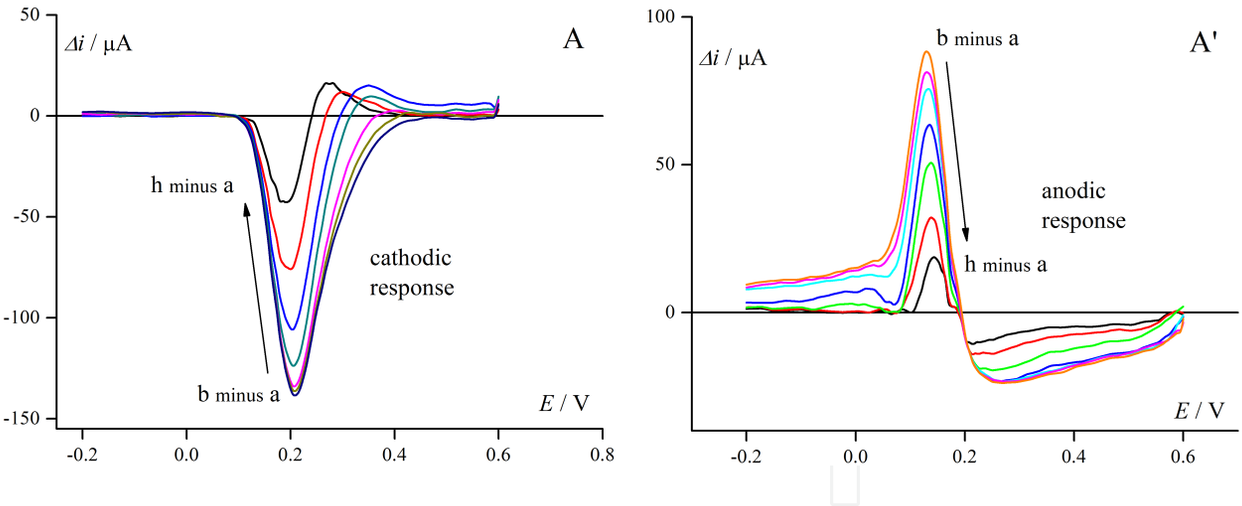

Figure 14. Another examples of CPR effect derived by digitalization and processing of literature CV data [14] (with kind permission from Wiley) for electroreduction of 1.0 mM 4-*tert*-butylcatechol in the presence of various concentrations of β-CD at pH 7.0. Concentration of β-CD from (a) to (h): 0.0, 0.3, 0.5, 1.0, 2.0, 4.0, 7.0, and 10.0 mM, respectively. Scan rate: 2 V s^{-1}.

Stochastic nature of adsorption phenomena is also visible on surface tension π vs. potential E dependences presented in monograph [15,16]. The *CPR* peaks involved in adsorption phenomena are similar to ones obtained by means of chromatography. The latter also

http://dx.doi.org/10.5772/53664

undergo Gaussian statistics [52]. Both facts confirm the probabilistic character of chemical dynamics [53].

4.4. CPR effects for auto-electrocatalysis processes (ACPR)

The hitherto presented data respected to the electroreduction of inorganic cations in the presence of non-electroactive organic adsorbate. Some experimental facts indicate that the idea of CPR can be extended on electroactive adsorbates. In paper [17] we have detected the autocatalytic effect caused by organic electroactive substance i.e. that which playes double role of organic adsorbate and electroactive substance. The autocatalytic effect was revealed by comparison of experimental and mathematical model responses as well as by comparison of results obtained on Hg (autocatalytic effect present) and GCE electrode (no autocatalytic effect).

In order to show more quantitative explanation of the influence of the autocatalytic effect on the enhancement the cathodic current observed on Hg electrode the difference between experimental and model curves will be shown in Fig. 15.

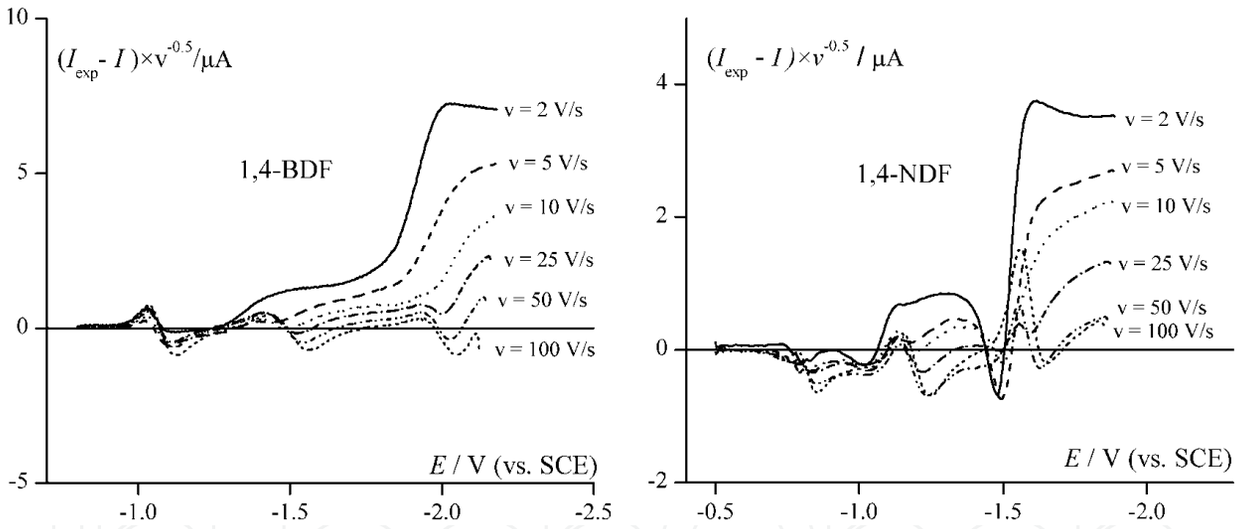

Figure 15. The "difference curves" (normalized vs. scan rate) between experimental (affected by adsorption) and model responses of the CV electroreduction of 1,4-BDF and 1,4-NDF in 0.3 M TBAP in DMF. The result can be considered as an example of auto-electrocatalytic effect. No smoothing of the data was applied. [Reprinted from *Electroanalysis*, Vol. 18, Sanecki, P., Skitał, P., Kaczmarski, K., Numerical Modeling of ECE – ECE and Parallel EE – EE Mechanisms in..., 981-991, Copyright (2006), with permission from Wiley].

From the character of the difference curves of CPR kind one may conclude that observed effect is not random but rather systematic with the wave profile increasing with the decreased scan rate. The observed autocatalytic effect vanish at high scan rates, giving discrepancy low enough to permit the usage of these data for the estimation of kinetic parameters [17]. If the effect is connected with adsorption of electrode reaction product, the adsorption process would be slow in comparison to the time window of the high scan rate experiment. Similar observations for inorganic reactant-organic substance/halide ion systems have been written

down by the others, by whom catalytic effect was explained by *bridging model* [49] or *surface reaction model* (see [54] and the literature cited therein).

Interesting electrocatalysis/electroinhibition examples of CPR type effects can be provided by early published polarographic data. Maxima of first kind (sharp) and second kind (diffused) appearing on diffusion/convection controlled limiting currents generally are explained by adsorption of electroactive substance and/or a movement of the solution near the electrode surface. Polarographic maxima were recognized as a case of electrocatalysis [5c, 55]. Since maxima hinder the precise evaluation of polarographic curves, they (maxima) are removed (damped) by introduction of strong surface active compounds as high-molecular organic compounds e.g. dyes (fuchsin). It means that a adsorption competition between electroactive adsorbate and nonelectroactive adsorbate takes place.

The adsorption of electroactive substance can be a source of its additional amount on electrode surface and consequently of limiting current excitation. Fig. 16 presents an example of such kind of auto-electrocatalysis, in which asymmetric curve, of autocatalytic CPR kind (ACPR), characteristic to first kind maximum, appears (source of data [55]).

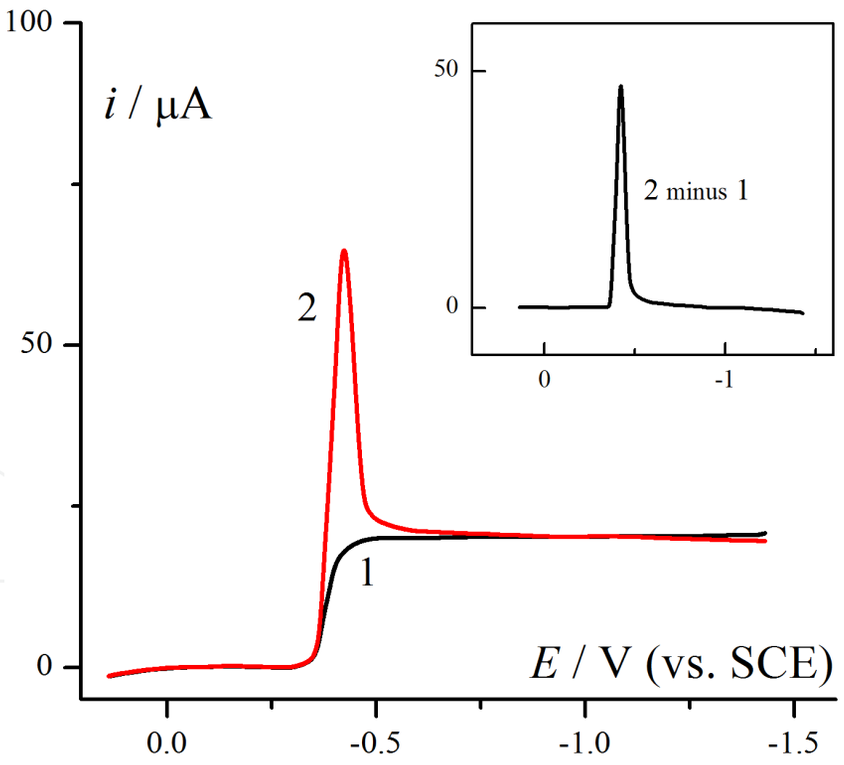

Figure 16. An example of electrocatalysis caused by adsorption of electroactive substance i.e. Pb^{2+} ions. The process can be considered as autocatalytic CPR effect (ACPR). The polarographic reduction of 2.3 mM Pb^{2+} in 0.1 M KCl solution: (curve 1) in absence of maximum suppressor; (curve 2) after the addition of 0.0002% sodium methyl red; inset window (curve 2 minus 1) i.e. affected curve minus regular curve. Curves 1 and 2 were obtained from processed data of Figure 6.8, p. 317 in [55].

http://dx.doi.org/10.5772/53664

The symmetric difference curve of ACPR kind can be obtained from second kind maxima data Fig. 17 ([5] Fig. XVIII-8, p.419).

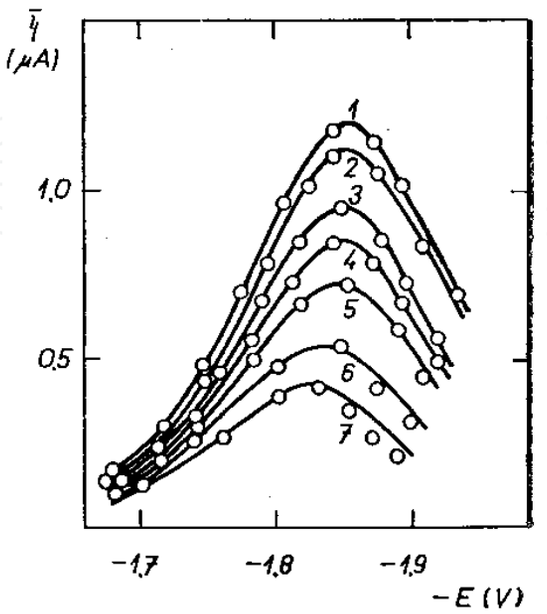

Figure 17. Another example of autocatalytic ACPR effect obtained from literature data [5]. The influence of ionic strength on catalytic hydrogen evolution waves in 3 mM solution of quinine in borate buffer pH 9.5. Concentrations of Na^+: (1) 0.04 M; (2) 0.045 M; (3) 0.05 M; (4) 0.055 M; (5) 0.06 M; (6) 0.07 M; (7) 0.08 M. [Reprinted from [5] Heyrovský, J.; Kůta, J. Principles of Polarography, Publishing House of the Czechoslovak Academy of Sciences: Prague 1965, Fig. XVIII-8, p.419].

The gradual passing from first kind maximum (a) to second kind maximum (f), presented in [5], can be interpreted as a change of adsorption mechanism visible as the change of shape of probabilistic curve (Fig. 18).

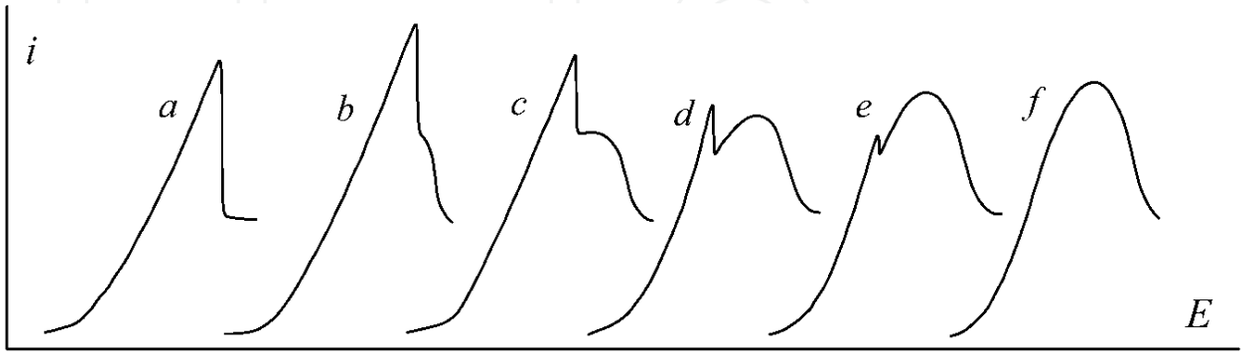

Figure 18. Another example of electrocatalysis of CPR type caused by adsorption of electroactive substance namely i.e. molecular oxygen. Solution 0.01 M KCl, exposed to air. The change of electrochemical response was caused by mercury head height lowering (processed literature data from Heyrovský, J.; Kůta, J. Principles of Polarography, Publishing House of the Czechoslovak Academy of Sciences: Prague 1965, Fig. XIX-23, p.457 [5].

On the other side, electroinhibition examples can also be recognized as characteristic minima on limiting currents of anions electroreduction e.g. $S_2O_8^{2-}$ (Figures XIV-17, XIV-21, XIV-22 in [5]). They also yield the difference curves of the symmetric probabilistic shape. Their precise explanation is much more complex and should be considered in frames of double layer structure changes.

5. Conclusions

1. The faradaic electrode process of electroreduction of inorganic cations creates a reference system on which the adsorption / inhibition effect can be observed.
2. The experimental catalysis/inhibition effect of electrode process affected by adsorption can be quantitatively separated from complex current response and displayed in the form of probabilistic type faradaic currents. The CPR curves can be considered as a quantitative adsorption characteristic of an electroinactive organic adsorbate. In many cases, the inhibition and catalysis processes are mutually coupled.
3. The results obtained by numerical simulation for EE process indicate that CPR effect is not accidental and that the assumption, that organic substance increases or decreases the apparent or individual rate constant of the electrode process, which is commonly accepted in literature is of value.
4. In the CPR presentation the effect of adsorption is separated and defined as well as can be processed and discussed quantitatively e.g. as a function of scan rate, a concentration of species in solution, etc. The shape of CPR curve (symmetrical or not symmetrical) may indicate the presence of possible interactions between molecules of adsorbate (Langumir or Frumkin model of isotherm).
5. The CPR effect is also observed for systems in which an organic or inorganic adsorbate is an electrode active reagent simultaneously (autocatalytic ACPR case).
6. Electrocatalysis/electroinhibition effect is a positive/negative difference between electrochemical response after and before introduction of a non-electroactive substance into solution and/or on electrode surface or a positive/negative difference between electrochemical response affected and non affected by substrate/product adsorption. The difference (eq. (2)) can be expressed quantitatively in the bell-shaped peak form of *Current Probabilistic Response*.

Abbreviations, symbols and acronyms

CPR – probabilistic type current response ("difference curves") obtained from eq. (2)

ACPR – autocatalytic CPR effect

CV – cyclic voltammetry

http://dx.doi.org/10.5772/53664

NPP – normal pulse polarography

EE – set of two consecutive one electron steps

α-CD – α-cyclodextrin

β-CD – β-cyclodextrin

SCE – saturated calomel electrode

TBAP – tetrabuthyl ammonium perchlorate

DMF – dimethylformamide

Q – charge

1,4-BDF – 1,4-benzenedisulfonyldifluoride

1,4-NDF – 1,4-naphthalenedisulfonyldifluoride

Tables

Adsorbate	Electrochemical. reaction, Electrode material	Figure	Observed effect	Literature
N,N'-dimethylthiourea, 3,4-diaminotoluene	$Zn^{2+} + 2e^{-} = Zn$, Hg	Fig. 1	CPR	this paper
n-pentanol		Fig. 2A, B	CPR	this paper
n-hexanol, *n*-pentanol, *t*-pentanol, *n*-butanol, *n*-propanol		Fig. 3A, B	CPR	this paper
α-cyclodextrin		Fig. 4A	CPR	this paper
β-cyclodextrin		Fig. 4B	CPR	this paper
α-cyclodextrin		Fig. 5	CPR	this paper
N,N'-dimethylthiourea		Fig. 7A	CPR	this paper
N,N,N',N'-tetramethylthiourea		Fig. 7B	CPR	this paper
dextran		Fig. 7C	CPR	this paper
N,N-dimethylaniline	$O_2 + e^{-} = O_2^{-\cdot}$, GCE	Fig. 7D	CPR	this paper
dextran	$Zn^{2+} + 2e^{-} = Zn$, Hg	Fig. 7E	CPR	this paper
3,4-diaminotoluene		Fig. 7F	CPR	this paper
thiourea		Fig. 7G	CPR	this paper
N,N'-dimethylthiourea		Fig. 7H	CPR	this paper
N,N'-diethylthiourea		Fig. 7I	CPR	this paper
N,N,N',N'-tetramethylthiourea		Fig. 7J	CPR	this paper

Adsorbate	Electrochemical. reaction, Electrode material	Figure	Observed effect	Literature
thiourea	$O_2 + e^- = O_2^{-\cdot}$, GCE	Fig. 8A	CPR	this paper
N,N-dimetyloaniline	$O_2 + 2e^- + 2H^+ = H_2O_2$, Hg	Fig. 8B	CPR	this paper
N-methylthiourea, N,N'-dimethylthiourea, N,N,N',N'-tetramethylthiourea	$Bi^{3+} + 3e^- = Bi$, GCE	Fig. 9	CPR	this paper
modeling via *k* variation	–	Fig. 10	CPR as a model effect	this paper
polyvinyl alcohol	$V^{4+} + e^- = V^{3+}$, Hg	Fig. 11	CPR	[5b]
Modification of electrode surface	photocurrent, p-Si electrode	Fig. 12	CPR	[51]
Modification of electrode surface	photocurrent, p-Si and p-Si-Me electrodes	Fig. 13	CPR	[51]
β-cyclodextrin	Electroxidation of 4-*tert*-butylcatechol (H_2Q) $H_2Q - 2e^- = Q + 2H^+$, GCE	Fig. 14	CPR	[14]
1,4-BDF	$ArSO_2F + 2e^- = ArSO_2^- + F^-$, GCE	Fig. 15	ACPR	[17]
1,4-NDF				
Pb^{2+} ions	$Pb^{2+} + 2e = Pb$, Hg	Fig. 16	ACPR	[55]
quinone	$H^+ + e = H$	Fig. 17	ACPR	[5]
O_2	O_2/H_2O_2, Hg	Fig. 18	ACPR	[5]

Table 1. The list of adsorbates and the electrode processes applied in the present study.

Author details

Piotr M. Skitał and Przemysław T. Sanecki*

*Address all correspondence to: psanecki@prz.edu.pl

Faculty of Chemistry, Rzeszów University of Technology, Rzeszów, Poland

This chapter is dedicated to professor Zbigniew Galus.

http://dx.doi.org/10.5772/53664

References

[1] Krjukova AA, Loshkarev MA. O prirode tormozyashchego deistviya poverkhnostno-aktivnykh-veshchestv na elektrodnye protsessy. Zh. Fiz. Khim. 1956;30: 2236–2243.

[2] Schmid R, Reilley CN. Concerning the effect of surface-active substances on polarographic currents. J. Am. Chem. Soc. 1958;80: 2087–2094.

[3] Weber J, Koutecký J, Koryta J. Ein Beitrag zur Theorie der polarographischen Ströme, die durch Adsorption eines elektroinaktiven Stoffes beeinflußt sind. Z. Elektrochem. 1959;63: 583–588.

[4] Weber J, Koutecký J. Theorie der durch die Adsorption des elektroinaktiven Stoffes bei einer reversiblen Elektrodenreaktion beeinflussten polarographischen Ströme. Collect. Czech. Chem. Commun. 1960;25: 1423–1426.

[5] Heyrovský J, Kůta J. Principles of Polarography. Prague: Publishing House of the Czechoslovak Academy of Sciences; 1965. a) p309. b) p315. c) p459.

[6] Sykut K, Dalmata G, Nowicka B, Saba J. Acceleration of electrode processes by organic compounds - "cap-pair" effect. J. Electroanal. Chem. 1978;90: 299–302.

[7] Saba J, Nieszporek J, Gugała D, Sieńko D, Szaran J. Influence of the mixed adsorption layer of 1-butanol/toluidine isomers on the two step electroreduction of Zn(II) ions. Electroanalysis 2003;15: 33–39.

[8] Marczewska B. Mechanism of the acceleration effect of thiourea on the electrochemical reduction of Zinc(II) ions in binary mixtures on mercury electrode. Electroanalysis 1998;10: 50–53.

[9] Sanecki P. A distinguishing of adsorption-catalyzed and regular part of faradaic current for inorganic cation-organic adsorbate system: propabilistic curves in cyclic voltammetry and normal pulse polarography. Electrochem. Comm. 2004;6: 753–756.

[10] Golędzinowski M, Kisova L, Lipkowski J, Galus Z. Manifestation of steric factors in electrode kinetics. Investigations of the deposition and dissolution kinetics of the Cd^{2+} /Cd(Hg) system in presence of adsorbed aliphatic alcohols and acids. J. Electroanal. Chem. 1979;95: 43–57.

[11] Jaworski RK, Golędzinowski M, Galus Z. Adsorption of α-, β- and γ-cyclodextrins on mercury electrodes from 1M $NaClO_4$ and 0.5M Na_2SO_4 aqueous solutions. J. Electroanal. Chem. 1988;252: 425–440.

[12] Golędzinowski M. The influence of α-, β- and γ-cyclodextrins on the kinetics of the electrode reactions in 1M $NaClO_4$ and 0.5M Na_2SO_4 aqueous solution. J. Electroanal. Chem. 1989;267: 171–189.

[13] Hromadova M, de Levie R. A sodium-specific condensed film of α-cyclodextrim at the mercury / water interface. J. Electroanal. Chem. 1999;465: 51–62.

[14] Rafiee M. Electrochemical Oxidation of 4-tert-Butylcatechol in the Presence of β-Cyclodextrin: Interplay between E and CE Mechanisms. Int. J. Chem. Kin. 2012;44: 507–513.

[15] Lipkowski J, Ross PN. (eds.) Adsorption Molecules at Metal Electrodes. New York: VCH Publishers; 1992.

[16] Ibach H. Physics of Surfaces and Interfaces. Berlin: Springer-Verlag; 2006.

[17] Sanecki P, Skitał P, Kaczmarski K. Numerical modeling of ECE-ECE and parallel EE-EE mechanisms in cyclic voltammetry. Reduction of 1,4-benzenedisulfonyl difluoride and 1,4-naphthalenedisulfonyl difluoride. Electroanalysis 2006;18: 981–991.

[18] Sanecki P, Skitał P, Kaczmarski K. An integrated two phases approach to Zn^{2+} ions electroreduction on Hg. Electroanalysis 2006;18: 595–604.

[19] Sanecki P, Amatore Ch, Skitał P. The problem of the accuracy of electrochemical kinetic parameters determination for the ECE reaction mechanism. J. Electroanal. Chem. 2003;546: 109–121.

[20] Sanecki P, Kaczmarski K. The Voltammetric Reduction of Some Benzene-sulfonyl Fluorides, Simulation of its ECE Mechanism and Determination of the Potential Variation of Charge Transfer Coefficient by Using the Compounds with Two Reducible Groups. J. Electroanal. Chem. 1999;471: 14–25. Erratum published in J. Electroanal. Chem. 2001;497: 178-179.

[21] Sanecki P. A numerical modelling of voltammetric reduction of substituted iodobenzenes reaction series. A relationship between reductions in the consecutive-mode multistep system and a multicomponent system. Determination of the potential variation of the elementary charge transfer coefficient. Comput. Chem. 2001;25: 521–539.

[22] Sanecki P, Skitał P. The cyclic voltammetry simulation of a competition between stepwise and concerted dissociative electron transfer. The modeling of alpha apparent variability. The relationship between apparent and elementary kinetic parameters. Comput. Chem. 2002;26: 297–311.

[23] Sanecki P, Skitał P. The Application of EC, ECE and ECE-ECE Models with Potential Dependent Transfer Coefficient to Selected Electrode Processes. J. Electrochem. Soc. 2007;154: F152–F158.

[24] Sanecki P, Skitał P. The electroreduction of alkyl iodides and polyiodides The kinetic model of EC(C)E and ECE-EC(C)E mechanisms with included transfer coefficient variability. Electrochim. Acta 2007;52: 4675–4684.

[25] Skitał P, Sanecki P. The ECE Process in Cyclic Voltammetry. The Relationships Between Elementary and Apparent Kinetic Parameters Obtained by Convolution Method. Polish J. Chem. 2009;83: 1127–1138.

[26] Sanecki P, Skitał P, Kaczmarski K. The mathematical models of the stripping voltammetry metal deposition/dissolution process. Electrochim. Acta 2010;55: 1598–1604.

[27] Skitał P, Sanecki P, Kaczmarski K. The mathematical model of the stripping voltammetry hydrogen evolution/dissolution process on Pd layer. Electrochim. Acta 2010;55: 5604–5609.

[28] Speiser B. Numerical simulation of electroanalytical experiments: recent advance in methodology. In: Bard AJ, Rubinstein I. (eds.) Electroanalytical Chemistry, A Series of Advances. New York: Marcel Dekker, Inc.; 1996. vol. 19.

[29] Britz D. Digital Simulation in Electrochemistry. Berlin: Springer; 2005.

[30] Gosser JrDK. Cyclic Voltammetry: Simulation and Analysis of Reaction Mechanisms. New York: VCH Publishers, Inc.; 1993.

[31] Bard AJ, Faulkner LR. Electrochemical Methods, Fundamentals and Aplications. New York: Wiley; 2001.

[32] Bieniasz LK. Towards Computational Electrochemistry - A Kineticist's Perspective. In: Modern Aspects of Electrochemistry. Conway BE, White RE. (eds) New York: Kluwer Academic Publishers; 2002. vol35. p135-195.

[33] Bieniasz LK, Britz D. Recent Developments in Digital Simulation of Electroanalytical Experiments. Polish J. Chem. 2004;78: 1195–1219.

[34] Lasia A, Bouderbala M. Mechanism of Zn(II) reduction in DSO on mercury. J. Electroanal. Chem. 1990;288: 153–164.

[35] Niki KK, Hackerman N. The effect of normal aliphatic alcohols on electrode kinetics. J. Phys. Chem. 1969;73: 1023–1029.

[36] Niki KK, Hackerman N. Effect of n-amyl alcohol on the electrode kinetics of the V(II)/V(III) and Cr(II)/Cr(III) systems. J. Electroanal. Chem. 1971;32: 257–264.

[37] Andreu R, Sluyters-Rehbach M, Remijnse AG, Sluyters JH. The mechanism of the reduction of Zn(II) for $NaClO_4$ base electrolyte solutions at the DME. J. Electroanal. Chem. 1982;134: 101–115.

[38] Van Venrooij TGJ, Sluyters-Rehbach M, Sluyters JH. Electrode kinetics and the nature of the metal electrode. The Zn(II)/Zn electrode reaction studied at dropping gallium and mercury (micro) electrodes. J. Electroanal. Chem. 1996;419: 61–70.

[39] Hush NS, Blackledge J. Mechanism of the Zn^{II}/Zn(Hg) exchange: Part 1: the Zn^{2+}/Zn(Hg) exchange. J. Electroanal. Chem. 1963;5: 420–434.

[40] Manzini M, Lasia A. Kinetics of electroreduction of Zn^{2+} at mercury in nonaqueous solutions. Can. J. Chem. 1994;72: 1691–1698.

[41] Fawcett WR, Lasia A. Double layer effects in the kinetics of electroreduction of zinc(II) at mercury in dimethylformamide and dimethylsulfoxide solutions. J. Electroanal. Chem. 1990;279: 243–256.

[42] Barański AS, Fawcett WR. Electroreduction of Alkali Metal Cations. Part 2. Effects of Electrode Composition. J. Chem. Soc. Faraday Trans. 1. 1982;78: 1279–1290.

[43] Fawcett R, Jaworski JS. Electroreduction of Alkaline-earth Metal Cations at Mercury in Aprotic Media. J. Chem. Soc. Faraday Trans. 1. 1982;78: 1971–1981.

[44] Golędzinowski M, Kišová L. Mechanizm rozładowania jonów Cd2+ z wodnych roztworów niekompleksujących elektrolitów w obecności i nieobecności zaadsorbowanych na elektrodzie substancji organicznych. In: Galus Z. (ed.) Adsorption on Electrodes and Inhibition of Electrode Reactions. Warsaw-Lodz: The materials of 4th Symposium of Polish Chemical Society; 1980. p75 (in Polish).

[45] Ikeda O, Watanabe K, Taniguchi Y, Tamura H. Adsorption effects of highly polarizable organic compounds on electrode kinetics. Bull. Chem. Soc. Jap. 1984;67: 3363–3367.

[46] Hurlen T, Eriksrud E. Kinetics of the Zn(Hg)/Zn(II) electrode in acid chloride solution. J. Electroanal. Chem. 1973;45: 405–410.

[47] Van der Pol F, Sluyters-Rehbach M, Sluyters JH. On the elucidation of mechanisms of electrode reactions by combination of A.C. and faradaic rectification polarography. Application to the Zn^{2+} /Zn(Hg) and Cd^{2+} /Cd(Hg) reduction. J. Electroanal. Chem. 1975;58: 177–188.

[48] Pérez M, Baars A, Zevenhuizen SJM, Sluyters-Rehbach M, Sluyters JH. Establishment of an EEC mechanism for the Zn^{2+} /Zn(Hg) electrode reaction. A dropping zinc amalgam microelectrode study. J. Electroanal. Chem. 1995;397: 87–92.

[49] Tamamushi R, Ishibashi K, Tanaka N. Polarographic study on the electrode reaction of zinc ion. Z. Physik. Chem. N. F. 1962;35: 209–221.

[50] Bhugun I, Savéant J-M. Self-inhibition in catalytic processes: cyclic voltammetry. J. Electroanal. Chem. 1996;408: 5–14.

[51] Szklarczyk M. Photoelectrocatalysis. In: Murphy OJ., Srinivasan S, Conway BE. (eds.) Electrochemistry in Transition. From the 20th to 21st Century. New York and London: Plenum Press; 1992. Chapter 15. p206 - Fig. 1 and p207- Fig. 3.

[52] Guiochon G, Lin B. Modeling for Preparative Chromatography. Amsterdam: Academic Press; 1994. Chapter IV.

[53] de Levie R. Stochastics, the basis of chemical dynamics. J. Chem. Educ. 2000;77: 771–774.

[54] Souto RM, Sluyters-Rehbach M, Sluyters JH. On the catalytic effect of thiourea on the electrochemical reduction of cadmium(II) ions at the DME from aqueous 1 M KF solutions. J. Electroanal. Chem. 1986;201: 33–45.

[55] Meites L. Polarographic Techniques. second edition. New York: John Wiley & Sons, Inc.; 1965.Chapter 6.